Manganese-Enhanced Magnetic Resonance Imaging and Studies of Rat Behavior: Transient Motor Deficit in Skilled Reaching, Rears, and Activity in Rats After a Single Dose of $MnCl_2$

Magnetic Resonance Insights
Volume 10: 1–13

DOI: 10.1177/1178623X17706878

Mariam Alaverdashvili[1,2*], Valerie Lapointe[1], Ian Q Whishaw[1] and Albert R Cross[1,3*]

[1]Department of Neuroscience, Canadian Centre for Behavioural Neuroscience, University of Lethbridge, Lethbridge, AB, Canada. [2]Department of Surgery, College of Medicine, University of Saskatchewan, Saskatoon, SK, Canada. [3]Department of Physics and Astronomy, University of Lethbridge, Lethbridge, AB, Canada.

ABSTRACT: Manganese-enhanced magnetic resonance imaging (MEMRI) has been suggested to be a useful tool to visualize and map behavior-relevant neural populations at large scale in freely behaving rodents. A primary concern in MEMRI applications is Mn^{2+} toxicity. Although a few studies have specifically examined toxicity on gross motor behavior, Mn^{2+} toxicity on skilled motor behavior was not explored. Thus, the objective of this study was to combine manganese as a functional contrast agent with comprehensive behavior evaluation. We evaluated Mn^{2+} effect on skilled reach-to-eat action, locomotion, and balance using a single pellet reaching task, activity cage, and cylinder test, respectively. The tests used are sensitive to the pathophysiology of many neurological and neurodegenerative disorders of the motor system. The behavioral testing was done in combination with a moderate dose of manganese. Behavior was studied before and after a single, intravenous infusion of $MnCl_2$ (48 mg/kg). The rats were imaged at 1, 3, 5, 7, and 14 days following infusion. The results show that $MnCl_2$ infusion resulted in detectable abnormalities in skilled reaching, locomotion, and balance that recovered within 3 days compared with the infusion of saline. Because some tests and behavioral measures could not detect motor abnormalities of skilled movements, comprehensive evaluation of motor behavior is critical in assessing the effects of $MnCl_2$. The relaxation mapping results suggest that the transport of Mn^{2+} into the brain is through the choroid plexus-cerebrospinal fluid system with the primary entry point and highest relaxation rates found in the pituitary gland. Relaxation rates in the pituitary gland correlated with measures of motor skill, suggesting that altered motor ability is related to the level of Mn circulating in the brain. Thus, combined MEMRI and behavioral studies that both achieve adequate image enhancement and are also free of motor skills deficits are difficult to achieve using a single systemic dose of $MnCl_2$.

KEYWORDS: Brain imaging in the rat, MEMRI, motor behavior, skilled hand use, skilled reach-to-eat movement, manganese toxicity, manganese, relaxation

RECEIVED: June 29, 2015. **ACCEPTED:** February 17, 2017.

PEER REVIEW: Four peer reviewers contributed to the peer review report. Reviewers' reports totaled 2225 words, excluding any confidential comments to the academic editor.

TYPE: Original Research

FUNDING: The author(s) disclosed receipt of the following financial support for the research, authorship, and/or publication of this article: This study is supported by NSERC DG #327364-06 (A.R.C.), Alberta Heritage Foundation for Medical Research and Canadian Institute Health Research/Heart and Stroke Foundation (M.A.), and Canadian Stroke Network (A.R.C. and I.Q.W.).

DECLARATION OF CONFLICTING INTERESTS: The author(s) declared no potential conflicts of interest with respect to the research, authorship, and/or publication of this article.

CORRESPONDING AUTHORS: Mariam Alaverdashvili, Department of Surgery, College of Medicine, University of Saskatchewan, 107 Wiggins Road, Saskatoon, SK S7N 5E5, Canada. Email: mariam.alaverdashvili@usask.ca; Albert R Cross, Department of Physics and Astronomy, University of Lethbridge, 4401 University Drive, Lethbridge, AB T1K 3M4, Canada. Email: albert.cross@uleth.ca

Introduction

Manganese-enhanced magnetic resonance imaging (MEMRI)[1] is an imaging tool for "functional mapping" of behavioral-relevant neural circuits at megascale (across many brain areas) that can be applied to restrained or freely behaving animals.[2–7] MEMRI is also reported to reveal brain cytoarchitecture,[8] function-specific neural pathways,[9–13] and function-relevant neural populations.[14,15] The unique property of Mn^{2+} is that it is transferred through voltage-gated Ca^{2+} channels in "excited" neurons leaving a relative accumulation of Mn^{2+} in neural populations that have recently contributed to behavior.[16,17] Accumulated Mn^{2+} reduces T_1 and T_2 relaxation time resulting an increase in signal or enhancement in the image. Throughout this article, we refer to image enhancement as the signal (and signal to noise) increase resulting from the accumulation of Mn^{2+}. There is a direct relationship between the local concentration of Mn^{2+} and the relaxation rate ($R1 = 1/T_1$). Thus, quantitative R1 (and R2) maps are proportional to Mn^{2+} concentrations and can visualize behavioral-relevant neural populations.[18]

A major drawback of MEMRI is Mn^{2+}-induced toxicity to visceral organs, eg, liver, heart, lungs, and kidneys,[19,20] and the central nervous system.[21–27] Although Mn^{2+} at high doses[20] is known to cause a Parkinson-like condition called manganism, the minimum dosage at which detectable effects on motor behavior occur is still an open question. With single infusion of Mn^{2+} for the purposes of imaging, many studies report the absence of serious behavioral abnormalities.[2,15] However, toxic effects also occur after the infusion of Mn^{2+} as an imaging contrast agent in laboratory animals.[4,21,28,29] Mn^{2+} is reported to accumulate in brain structures involved in motor

* M.A. and A.R.C. are equal co-authors.

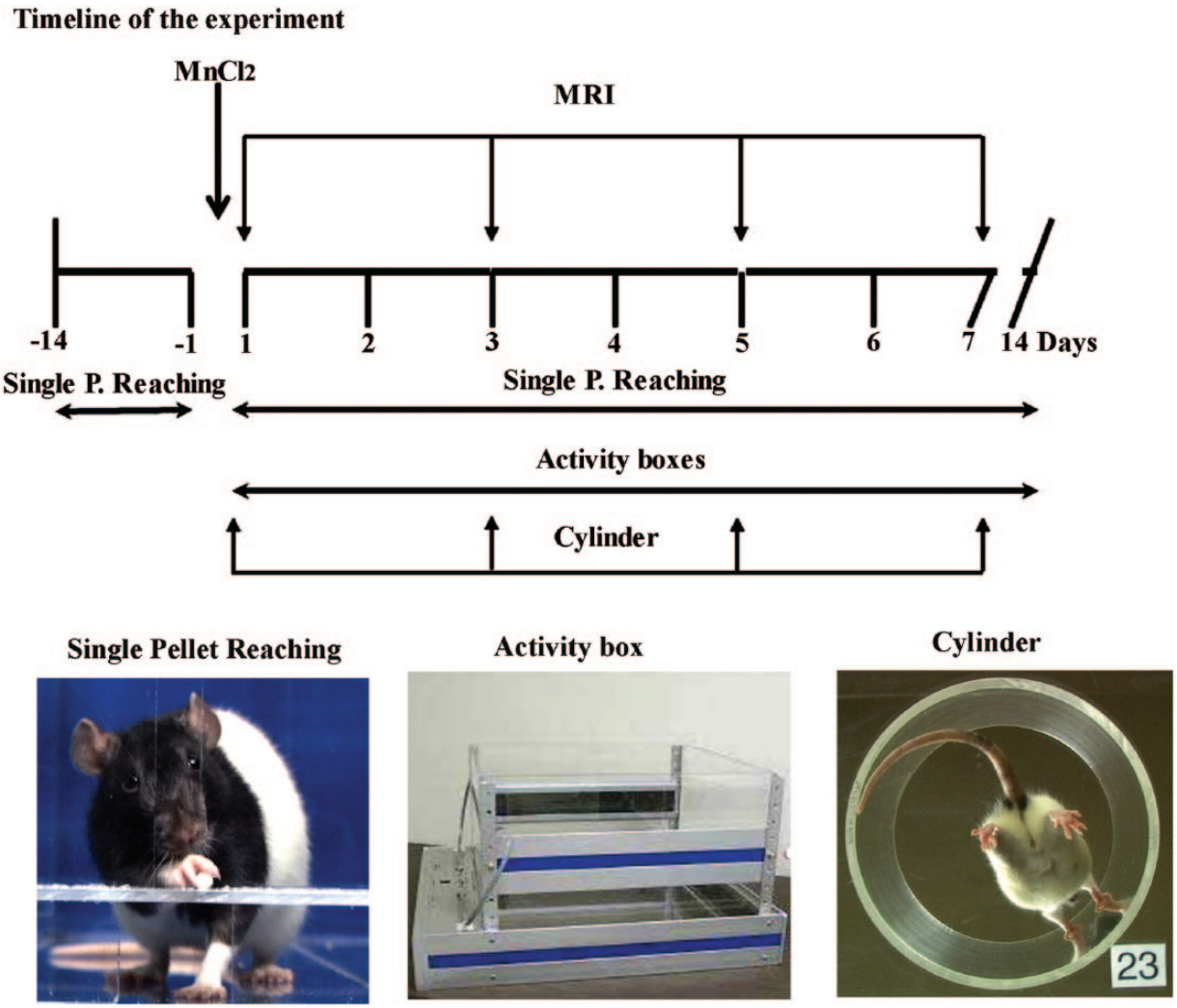

Figure 1. Experimental timeline (upper panel). The infusions ($MnCl_2$ or saline) took place at day 0 as indicated by the arrow. Behavioral apparatus (bottom panel)—single pellet reaching task evaluates skilled forelimb use, activity cage assesses locomotion and vertical exploratory activity/balancing ability, cylinder task assesses balancing ability. MRI indicates magnetic resonance imaging. P indicates pellet.

control including striatum and basal ganglia and motor cortex.[30,31] There are reports of motor abnormalities[32,33] with low chronic ingested or inhaled exposures of Mn^{2+}. More detailed behavioral studies have mixed findings. One study shows detectable motor abnormalities in wheel running,[4] whereas another reports the absence of abnormalities in swimming.[6] A follow-up running wheel study[34] shows a lack of abnormalities with the use of a continuous-delivery osmotic pump. There are a growing number of studies[35] comparing functional imaging with blood oxygen level–dependent and MEMRI methods.

MEMRI methods have the advantage that the functional task takes place outside of the magnet and is more natural for rodents. With a growing interest in functional methods, a careful investigation of the interaction of the MEMRI methods and behavioral tasks is necessary.

The purpose of this study was to investigate further the potential of combining MEMRI with various measures of motor behavior to determine the time frame of potential toxicity. The rats were given behavioral tests (Figure 1) of skilled hand use in reaching for food,[36,37] activity in an open field,[38] and balance in a cylinder test.[39] A moderate imaging dose was used, and behavior was tested before and after $MnCl_2$ infusion. The present sensitive measures of fine motor skills and balance have not been previously reported in conjunction with $MnCl_2$ infusion.

Materials and Methods

A total of 30 female, young adult (90-100 days old) Long-Evans hooded rats, from both the University of Lethbridge animal colony and Charles River Breeders (Lachine, Quebec), were used. The rats were assigned to naïve (n = 6), saline (n = 9), and $MnCl_2$ (n = 15) groups. Some rats in the $MnCl_2$ group (n = 11) received 48 mg/kg (1.11 mL), whereas others received (n = 4) 95 mg/kg (2.22 mL) of $MnCl_2$ solution. Saline group received an equivalent volume of saline (1.11 mL). Naïve rats were not exposed to any injections. The experiments were conducted in compliance with the guidelines and approval of

the "University of Lethbridge Animal Care Committee" (Institutional Ethical Committee). The "University of Lethbridge Animal Care Committee" follows the standards for the ethical use and care of animals in science of the "Canadian Council for Animal Care" which reflect international guidelines. The rats were housed in Plexiglas cages (36-cm long, 20-cm wide, and 21-cm deep) with sawdust bedding. Each cage contained groups of 2 or 3 rats. The cages resided in a colony room that was maintained on a 12 hours light/12 hours dark cycle (08:00–20:00 hours) with controlled temperature and humidity. Behavioral testing took place between 09:00 and 13:00 hours, in experimental rooms with controlled temperature and humidity.

The timeline of behavioral testing, infusions ($MnCl_2$ or saline), and magnetic resonance imaging (MRI) is shown in Figure 1.

Skilled reach-to-eat movement

The procedures used to acquire and analyze the single pellet reaching data follow those of Moon et al.[40] The elements that are relevant to this work are highlighted.

Single pellet reaching box. Single pellet reaching boxes[37] were constructed from clear Plexiglas (35 cm × 14 cm × 45 cm). The center of the front wall of the box had a vertical slot 1-cm wide that extends from 2 cm above the floor to a height of 15 cm. On the outside of the wall, in front of the slot, a 2-cm-wide shelf was mounted 3 cm above the floor. Two indentations to hold the food targets were located 2 cm from the inside of the wall and aligned with the edges of the slot (Figure 1, bottom panel).

Feeding and food restriction. The rats were motivated to reach by gradually restricting their food intake such that they maintained a body weight between 90% and 95% of normal. This was achieved by allowing access to a fixed daily ration (19-20 g per rat per day) of Purina rat chow prior to and during training. During the week prior to training, each rat received 20 dustless precision pellets of 45 mg (product #F0021; BioServe Inc., Frenchtown, NJ, USA) each day 1 hour prior to the daily ration. This familiarized the rats with the food used as the reaching target.

Video recording. Reaching performance was recorded using a Sony DCR-VX1000 3CCD camcorder (shutter speed: 1000/s) under a cold light. A Sony videocassette recorder (DSR-11) was used for subsequent frame-by-frame analysis. Representative still frames (Figure 1, lower left and right) were captured from digital video recordings with Final Cut Pro HD (V.4.5; http://www.apple.com).

Training. The initial pretraining sessions (10 minutes) took place daily. In these sessions, the rats were allowed to retrieve the pellet from the shelf with the mouth and tongue, aimed to familiarize the rat with food being available on the shelf for eating. To encourage the use of a paw, the pellets were moved further away as the animals learned to retrieve them. Once the rats demonstrate a preference for 1 paw, individual pellets were placed into the indentation contralateral to that paw. Because the rats pronate the paw lateral to medial, the pellet placement permits the use of only the preferred paw. During the second week of training, the rats received daily (~10 minutes) sessions of discrete trials. During intertrial intervals, the rats were shaped to leave the slot, walk to the rear wall of the cage, turn, and approach the slot again for the next pellet. In addition, by withholding food pellet on semirandomly selected trials, the rats were taught to sniff the shelf for a pellet and to reach only if a pellet was present. Thus, each rat eventually orients to the food pellet, transports its paw through the slot, grasps the food pellet, and retracts its paw through the opening to release the food into its mouth.[41]

After 2 to 3 weeks, each rat was given 20 daily trials until group success levels exceeded 50%. The rats then received $MnCl_2$ and testing of all rats recommenced 24 hours later. After infusion, the rats were retested in reaching for single pellets daily for the first week and then on day 14.

End-point analysis of reaching behavior. Reaching behavior was analyzed by measures of the following:

1. *First trial success*. First trial successes were ones in which a rat obtained a food pellet on the first advance of the paw toward the food. First trial success % = (number of pellets obtained on first advance/20)*100.
2. *Total success*. A successful reach was defined as one in which an animal grasped a food pellet and placed it into its mouth independent of the number of attempts. Success % = (number of pellets obtained/20)*100.
3. *Total reaching attempts*. Total reaching attempts included all movements of the paw through the slot independent of success.

Movement analysis of reaching behavior. The biometric measures of reaching action were scored before and after $MnCl_2$ infusion. Scoring was based on a conceptual framework derived from Eshkol-Wachman movement notation (EWMN).[37,42] Eshkol-Wachman movement notation describes the position of individual limbs, the trunk, the snout, and the head in relation to the food pellet with the body treated as a system of articulated axes (ie, limb segments, trunk axis, and snout axis). The following movements were scored[36]:

1. *Orient*. The head and the snout are oriented toward the target so that that rat sniffs the target.
2. *Limb lift*. The paw is raised from the floor until the digits are aligned with the midline of the body.
3. *Digits close*. The palm is supinated so that it is oriented vertically, and the digits are semiflexed.
4. *Aim.* The elbow is adducted to the body midline with a movement of the upper arm, whereas the digits remain positioned on the body midline.

5. *Advance*. The forelimb moves forward through the slot.
6. *Digits extend and open*. The digits are extended as the limb is advanced and then are opened as the paw is pronated over the food.
7. *Pronate*. The elbow abducts with a movement of the upper arm pronating the paw over the target in an arpeggio movement.[43]
8. *Grasp*. The arm remains still, whereas the digits close to grasp the food and then the paw is extended and raised.
9. *Supinate I*. The paw is supinated by 90° by abducting the elbow so that the paw holding the food can be withdrawn through the slot.
10. *Supinate II*. The paw is supinated so that the palm faces the mouth.
11. *Release*. The food pellet is released into the mouth by opening the digits.
12. *Replace. T*he paw is placed on the floor surface (or sometimes the rat may rear and place the paw on the wall) with all digits extended.

Each of these movement elements was rated using a 3-point scale. A score of "1" indicated that the movement was normal. A score of "1.5" was awarded to a movement that was present but abnormal. A score of "2" meant the movement was absent.

Scoring was achieved by stepping through the video record frame by frame (30 f/s) and applying a score to each of the movements for the first 3 successful reach with first attempt. The movement scores were then averaged for selected reaching actions to calculate the total movement score.

Kinematics of reaching behavior. $MnCl_2$ effects on the kinematics of reaching movement were assessed by the time required to execute the individual gestures during the reaching action. Gestures of the forelimb in skilled reaching[44,45] were identified by their trajectories, by the pauses, and changes in trajectory that occur between them or by their repetitions:

1. *Advance*. A gesture in an advance begins with the paw lifted from the floor. The forelimb moves through the slot, to approach the food, and may or may not include a return toward the mouth.
2. *Grasp*. A grasp begins with the paw moving toward the food target and ends as the digits flex and close in an attempt to grasp the pellet.
3. *Withdrawal*. A gesture in a withdrawal begins with a movement of the forelimb away from the apparent location of the food to bring the paw to the mouth.
4. *Release.* A release withdraws the paw from the mouth to return it to the floor or redirects the paw to the advance.

In this study, the time required to execute advance, withdrawal, and release was compared between the groups before and after $MnCl_2$ infusion.

Motor performance index. Total movement scores were normalized with preinfusion performance (performance index [PI]) to avoid a confounding effect from the baseline (ie., biological) variability in qualitative aspects of reach-to-eat action. The PI was calculated as the postinfusion score divided by the preinfusion score for each rat.[40]

Activity measures

Daily activity of $MnCl_2$, saline, and naïve rats was acquired using a VersaMax Animal Activity Monitoring System (AccuScan Instruments, Inc., Columbus, OH, USA; https://www.alnmag.com/company-profiles/accuscan-instruments-inc). The rat's spontaneous activity was first examined in the open field (square area with the walls (42.5 cm × 42.5 cm × 30 cm; Figure 1, bottom panel) at 24 hours after infusion ($MnCl_2$ or saline). During the first postinfusion week, spontaneous activity was measured daily and on day 14 after infusion. The rats were not exposed to the activity box prior to the infusions to ensure that novel environment exploration activity took place. Activity was measured as total distance and the number of rears during each 30-minute session.

Cylinder test

The balancing ability of the rats during vertical activity was examined in the cylinder test[39] (Figure 1, bottom panel). Rats were individually placed in a transparent Plexiglas cylinder (20 cm in diameter and 30 cm in height) for 5 minutes. When put in a cylinder, a rat spontaneously rears up to explore the cylinder and the wall of the cylinder. The rat rears either with or without the support of the body by the forepaws. The cylinder was located on a transparent table with a mirror placed directly underneath the table and tilted at an angle to allow filming of the rats from a ventral view. Balancing ability was measured as the number and time of vertical exploratory activity with and without supporting the body by leaning with forepaws on the wall.

Magnetic resonance imaging

MRI contrast agent, dose, and the route of administration. The choice of $MnCl_2$ dose and the route of administration were based on previous findings, the efficacy of contrast for imaging,[46,47] and the least adverse effect on motor behavior and visceral organs.[48] Intravenous infusion was used because this delivery leads to rapid transport to the nervous system[31,49–51] while minimizing adverse effects on visceral organs.[19,20] The dose of $MnCl_2$ used for all of the rats was 48 mg/kg. The rats were given a single dose of $MnCl_2$ via a tail vein infusion. For greater image enhancement, a higher dose (95 mg/kg) was attempted on a small number of animals. All of these animals died during or within 2 days of infusion. Because our goal was to achieve image enhancement with a dose that minimally affected behavior, this part of the experiment was stopped. Thus, behavioral testing was only performed on the naïve, saline, and 48 mg/kg $MnCl_2$–injected rats.

Manganese preparation and infusion. The preparation of the manganese stock solution was based on the procedures outlined in the work by Silva.[29] Specifically, NaOH was added to a 100-mM solution of Bicine in double-distilled water (ddH_2O) to adjust the pH to about 8.5. The amount of $MnCl_2$ powder to achieve a 120-mM solution was then added. This addition lowered the pH to about 6.5. The final pH of 7.4 was obtained by slowly adding drops of a NaOH solution (10 pellets in 10 mL ddH_2O). This procedure resulted in a clear amber colored solution with no visible precipitates.

A syringe pump (Pump 11 Elite; Harvard Apparatus; http://www.harvardapparatus.com) was used to infuse either 1.11 mL (48 mg/kg in 350 g rate) or 2.22 mL (95 mg/kg in 350 g rat) of the solution into the tail vein at a rate of 1.06 mL/h. The delivered dose of 48 mg/kg of $MnCl_2$ corresponds to 20.8 mg/kg of Mn^{2+} (the exact dose of 47.7 mg/kg has been rounded to 48 mg/kg for brevity). During manganese administration, anesthesia was maintained with about 1% isoflurane anesthesia. During $MnCl_2$ infusion, Po_2 and respiration, heart rate, and oxygen saturation were carefully monitored using the MouseOx (STARR Life Sciences Corp.) and maintained at 40 to 48 breathes/min, 250 to 320 beats/min, and 96% to 98% of oxygen, respectively. The rectal temperature was monitored and kept constant at 37°C ± 0.5°C using a homeothermic blanket system (www.harvardapparatus.com).

MRI equipment and imaging protocol. The images were acquired using an MRI scanner consisting of a 4.7-T 330-mm bore Oxford magnet (Oxford, UK) and an SMIS MR 5000 (Surrey, UK) console. The imaging gradients were an Oxford self-shielded gradient set capable of 15 G/cm driven by Techron amplifiers (initially, model 7550 upgraded to model 7780). The imaging coil was a homebuilt 8-rung quadrature birdcage design that was 52 mm in diameter and 54 mm in length. The hybrid coupler used to combine the quadrature channels was an Anaren model 10012-3, and the preamplifier was a MiteQ model AU-1466. Sets of crossed diodes and λ/4 cables were inserted between the hybrid and the pre-amp for passive separation of the low power from the high-power radio frequency (RF).[52] A 300-W broadband RF amplifier (AMT Model M3206) was used. An MRI-compatible Stereotaxis (Kopf, CA) was used to position the animals with the ear bars passing through holes in the cylinder of the custom-built MRI coil. The imaging protocol for each rat consisted of the following: (1) 3 multislice localizer spin echo [SE] image sets (repetition time [TR]: 600 ms, echo time [TE]: 42 ms, 0.3 mm × 0.3 mm × 1.6 mm) in coronal, axial, and sagittal orientations; (2) a single-slice saturation recovery spin-echo T_1 measurement (8 saturation delays 3000, 2000, 1200, 850, 600, 400, 300, 150; TE: 22 ms, 0.5 mm × 0.5 mm × 1.6 mm) in the sagittal directions; and (3) the same single-slice T_1 measurement in the coronal direction; and (4) a 3-dimensional (3D) T_1-weighted gradient echo (TR: 100 ms, TE: 7 ms, θ: 70°, 0.6 mm × 0.6 mm × 0.6 mm) acquisition sequences. The total imaging time of the protocol was about 1 hour. The sagittal T_1 measurement was prescribed to be along the midline of the brain using the localizer images. The coronal T_1 measurement was acquired on a slice located at the bregma.[53] The 3D acquisition used a 12-mm coronal slice centered about the hippocampus. The 3D field of view (FOV) was 76 mm × 76 mm with a 19-mm FOV in the slice direction. The 3D acquisition was 128 × 128 × 32 to give a 0.6-mm isotropic voxel acquisition. Each dimension was zero filled during processing to give 0.3-mm isotropic voxels in the final registered images. Reference samples (ie, phantoms) containing 0.12, 0.11, and 0.10 mM $MnCl_2$ were placed above the brain for standardization and quality control. The samples were selected to give a T_1 of ~900, 950, and 1000 ms. gas anesthesia (isoflurane) was used during the imaging sessions. T_1 values were calculated for each pixel in the image using home-written software written in IDL (ITT, Boulder, CO, USA) to produce T_1 maps. Regions of interest for various anatomical structures were manually extracted from the T_1 maps with Analyze 11.1 (BIR, USA). Registration was performed with the 3D voxel registration tool of Analyze 11.1.

Statistical analysis

Statistical analysis was performed using SPSS 13. Data were treated as interval data according to the definition of Field and Hole.[54] Results for end-point measures (success, success on the first reaching attempt), spontaneous activity, and balancing capability were analyzed using mixed-design repeated measures analysis of variance, "days" used as the within-subjects variable, and "groups" as the between-subjects factor. The Mauchly test and Greenhouse-Geisser corrections were used to correct data sphericity. Comparisons between groups were performed by follow-up Bonferroni test. Dependent (paired-samples) *t* tests were used to compare pre- and postcontrast reaching performance.

Movement elements were analyzed using nonparametric tests (Mann-Whitney *U* and Kruskal-Wallis). Wilcoxon signed ranked *t* test (*z* statistics) followed by the Bonferroni correction was used for multiple follow-up comparisons between pairs of conditions.

The difference in the relaxation rate in brain regions and pituitary gland between groups was determined by independent *t* test. The Levene test for equality of variance was run to check the assumption of homogeneity of variance, and the degree of freedom was corrected in accordance with the test result. To assess whether the relaxation rate in pituitary gland and behavior was related, correlative (bivariate) analysis was performed between the relaxation rate and behavioral measures. Moreover, the Pearson (*r*) and Spearman (ρ) correlative analysis was conducted between relaxation rate and motor performance indices of skilled reaching action. For all analyses, significance was considered to be a *P* value less than .05.

Results

All rats survived after $MnCl_2$ infusion through the tail vein at the dose 48 mg/kg. General observation of grooming and

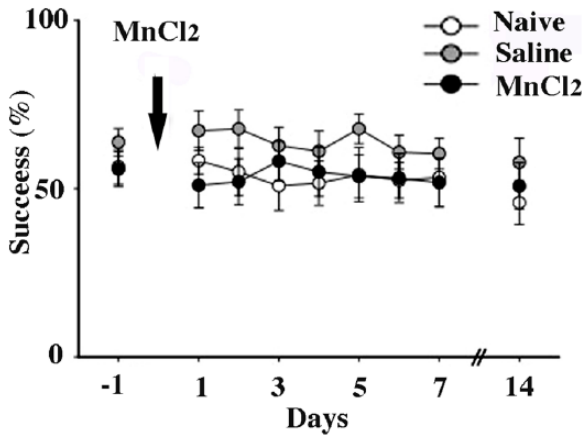

Figure 2. Successful reaches made by rats (mean ± SEM) in a single pellet reaching task. The infusions ($MnCl_2$ or saline) took place at day 0 as indicated by the arrow. Note that $MnCl_2$ infusion slightly reduced success on day 1, but the change is not significant.

home cage activity indicated that these rats tolerated the procedure well. The initial recovery from anesthesia was not noticeably different from the saline-infused group, and the rats were ready for behavioral testing within 24 hours of the $MnCl_2$ infusion. The data below and following discussion were based on the 48 mg/kg dose of $MnCl_2$. In the MEMRI literature, systemic doses from 5 to 175 mg/kg[29] have successfully been used for MRI image enhancement, and thus, the Mn^{2+} amount is referred to below as a moderate imaging dose.

Skilled reach-to-eat movement

End-point measures

Success. A summary of reaching success scores for naïve, saline, and $MnCl_2$ groups is illustrated in Figure 2. There was no adverse effect of the moderate dose of $MnCl_2$ on the success level either acute or in the chronic post-$MnCl_2$ period. Repeated measures analysis of variance did not give significant difference among groups ($F_{2,23}$ = 1.09; P > .05), testing days ($F_{4.1,94.7}$ = 1.37) or group by day interaction ($F_{8.2,94.7}$ = 0.70; P > .05).

Success on the first reaching attempts. There was no difference among groups for the more demanding measure of skilled reach success on the first reach. Repeated measures analysis of variance gave no group ($F_{2,23}$ = 0.37; P > .05), day ($F_{3.8,86.9}$ = 1.52; P > .05), or day by group effect ($F_{7.6,86.7}$ = 1.24; P > .05).

Reaching attempts. Number of reaching attempts was also similar between naïve, saline, and $MnCl_2$ groups following infusion. There was no group ($F_{2,23}$ = 0.58; P > .05), day ($F_{2.7,56.5}$ = 1.46; P > .05), or day by group effect ($F_{4.9,56.5}$ = 0.86; P > .05).

Biometric measures of reaching movement. Prior to $MnCl_2$ administration, there was no difference between rats assigned to be naïve, saline, and $MnCl_2$ groups for any movement elements of reaching (P > .05). Significant abnormal reaching movements were observed 24 hours after $MnCl_2$ administration in the $MnCl_2$ group compared with naïve and saline groups (total movement scores: $\chi^2(2)$ = 13.8; P < .001). The group differences originated mainly from the statistically significant difference in supination II and release (Table 1).

Table 1. Group differences in movement elements in a single pellet reaching task before and 24 hours after $MnCl_2$ infusion.

MOVEMENT ELEMENTS	NAÏVE VS $MNCL_2$	SALINE VS $MNCL_2$
Supination II	U = 12*	U = 13**
Release	U = 6*	U = 9.5**
Other movement elements	ns	ns

*$P \leq .05$; **$P \leq .01$; ns: $P > .05$.

There was a statistically significant difference in skilled paw use after $MnCl_2$ infusion compared with pre-$MnCl_2$ behavior, but the difference was observed only at 24 hours after $MnCl_2$ infusion (Figure 3B). Wilcoxon signed rank tests (followed by the Bonferroni correction) between pairs of conditions (pre-$MnCl_2$ vs day 1—$MnCl_2$) yielded statistically significant difference in total movement scores (T = 1, z = −2.85; P < .004). The difference stemmed from the $MnCl_2$ effect on supination II (T = 1, z = −2.71; P < .007) and release (T = 0, z = −2.67; P < .007) (Figure 3A).

Kinetics of reaching gestures. $MnCl_2$ slowed down the reaching gestures, especially the gestures that bring the grasped pellet to the mouth (Table 2).

The grasp lasted less than 1 ms both before and after $MnCl_2$ administration. The comparison of grasp time was not significant; however, these movements are at the limit of the timing sensitivity.

Activity measures

A summary of the $MnCl_2$ effect on gross motor behavior in activity cages is shown in Figure 4. $MnCl_2$ infusion significantly reduced both horizontal (the distance) (Figure 4A) and vertical (rearing) activity (Figure 4B). The effect was transient and returned to normal levels by day 4. Repeated measures analysis of variance for the distance moved gave significant day ($F_{3.7,85.9}$ = 4.15; P < .05) and day by group effect ($F_{7.5,85.9}$ = 2.77; P < .05). Group effect ($F_{2,23}$ = 1.89; P > .05) was not significant. The planned comparison yielded statistically significant differences between the $MnCl_2$ and both saline and naïve groups on days 1 and 3 (P < .05) following $MnCl_2$ infusion. Repeated measures analysis of variance for rearing activity yielded significant group effect ($F_{2,23}$ = 4.55; P < .05), day effect ($F_{3.5,81.2}$ = 4.91; P < .05), and day by group effect ($F_{7.06,81.2}$ = 2.68; P < .05). Bonferroni test yielded statistically significant difference between $MnCl_2$ and both saline and naïve groups on days 1 and 3 (P < .05) following $MnCl_2$ infusion.

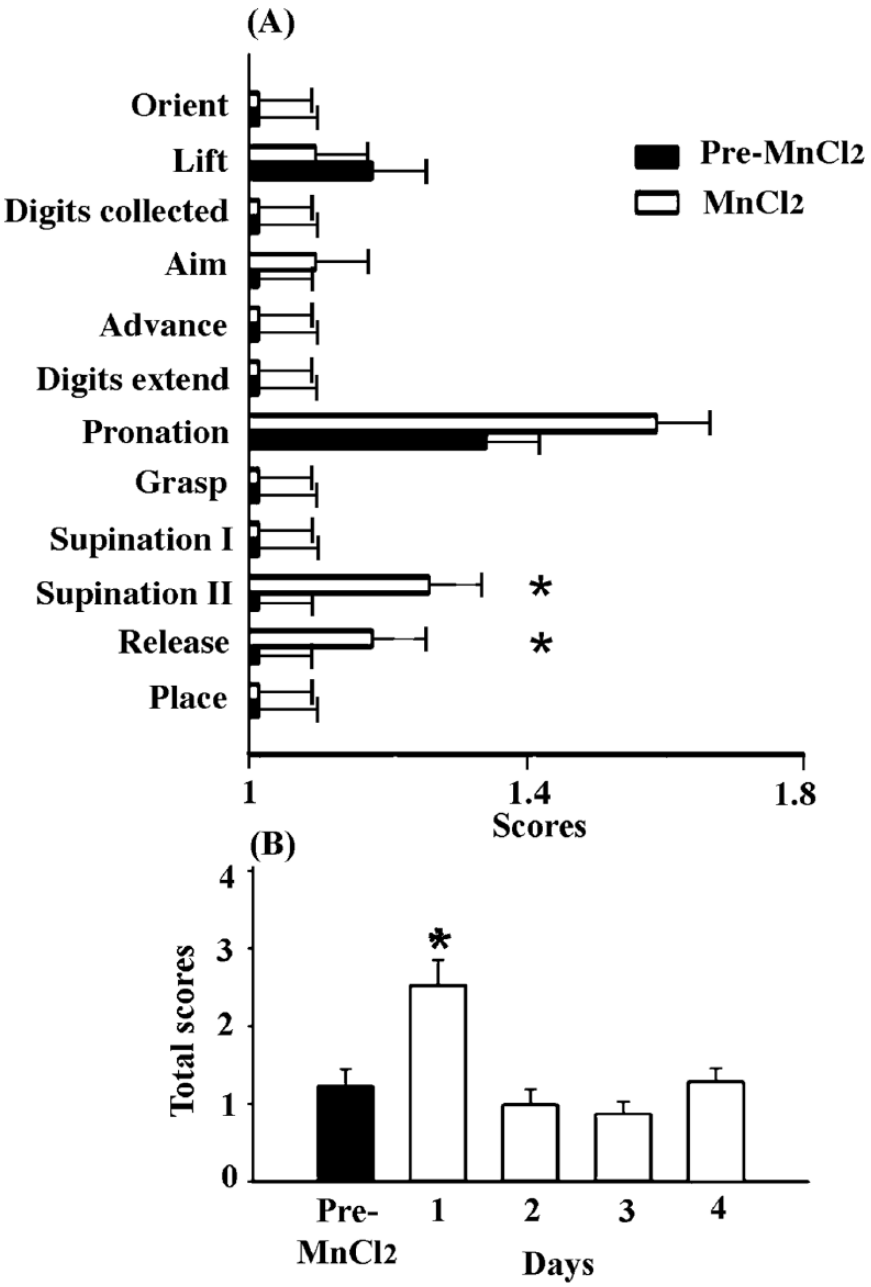

Figure 3. (A) Movement elements of skilled reaching action a single pellet reaching task before and 24 hours after infusion. Note significant abnormalities on "supination II" and "release." (B) Total scores of all movement elements of skilled reaching. $MnCl_2$-induced deficit in skilled reaching was transient and recovered on the second day after $MnCl_2$ infusion. Lower scores correspond to normal movement; high scores—affected movement. Asterisks denote significant group differences ($P < .05$).

Table 2. Duration of the reaching gestures in a single pellet reaching task before and 24 hours after $MnCl_2$ infusion.

REACHING GESTURES	PRE-$MNCL_2$, MEAN ± SD	24 H POST-$MNCL_2$, MEAN ± SD
Withdraw paw to mouth	15.15 ± 1.82 ms	21 ± 2.62 ms*
Release	17.33 ± 2.50 ms	50.79 ± 12.33 ms*
Transport	5.72 ± 0.35 ms	6.27 ± 0.46 ms (ns)

*$P \leqslant .05$; ns—$P > .05$.

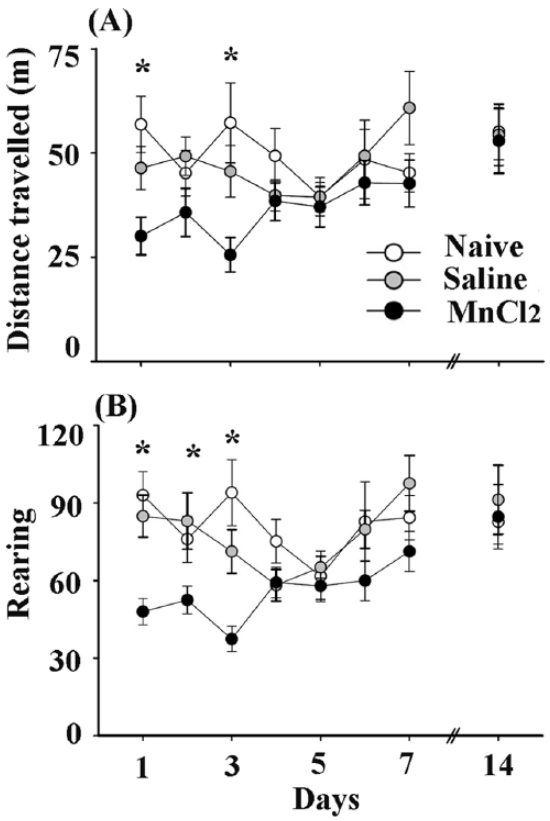

Figure 4. (A) Total locomotion and (B) rearing activity over the 30-minute session in the activity cages (mean ± SEM) after infusion. Note that $MnCl_2$ induced a transient reduction in motor activity in measures of gross motor behavior. Asterisks denote significant group differences ($P < .05$).

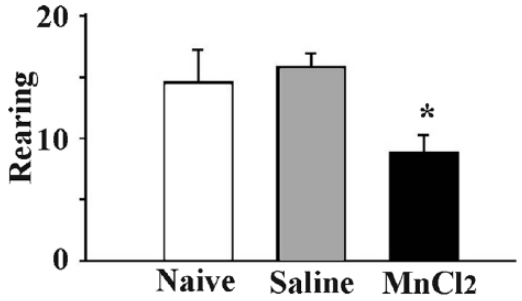

Figure 5. Cylinder task: the total number of unsupported rears over the 5-minute session, 24 hours after infusion. The asterisk denotes a significant difference ($P < .05$) between groups.

Cylinder

$MnCl_2$ significantly reduced vertical activity ($F_{2,23} = 21.23$; $P < .001$) compared with naïve ($P < .001$) and saline ($P < .001$) groups only at 24 hours after infusion. This difference stemmed from the reduction in the number of rears performed without support against the cylinder wall (group effect: $F_{2,23} = 12.25$; $P < .001$) compared both with naïve ($P < .001$) and saline groups ($P < .001$) (Figure 5) and the number of rears with the contact of the wall of the cylinder by the $MnCl_2$ group compared with naïve ($P = .013$) group.

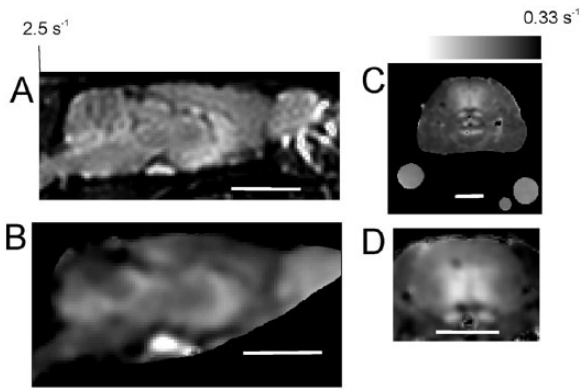

Figure 6. Representative R1 maps of 1 rat brain 24 hours after infusion. (A) sagittal plane, (C) coronal plane. "Mn distribution" map from the group-averaged difference between $MnCl_2$-injected and saline-injected rats. (B) sagittal plane, (D) coronal plane. Note the highest signal in the pituitary gland and the crescent-shaped intensity that follows the ventricles in A and B. Map D only shows the coronal brain region as the water samples in C varied in location from animal to animal and did not coregister. The horizontal color bar at the top indicates the colors that correspond to the R1 values with the maximum and minimum values indicated. Note that the gray level has been windowed to best reveal the R1 pattern, and the range of values extends from the black to the black line on the white end of the color bar. The white line on each image indicates 1 cm in distance.

MRI measures

R1 maps and 3D MRI. As was expected based on other literature,[29] the moderate dose of $MnCl_2$ significantly ($P < .05$) enhanced relaxation rates ($1/T_1$ or R1) throughout the brain compared with the saline group 24 hours after infusion. Significant increases in relaxation rates were found for up to 5 days in the cortex and up to 3 days in subcortical portions of the limbic system, brain stem, cerebellum, and pituitary gland ($P < .05$). The calculated R1 relaxation rate has a linear relationship with manganese concentration. Thus, the difference between a $MnCl_2$ infused and non-$MnCl_2$–infused R1 map will be directly proportional to Mn concentration and account for the baseline tissue R1. Assuming that the regional relaxivity is unchanged, the Mn^{2+} distribution map will be the result. Figure 6A shows a representative image from the sagittal R1 map of one of the manganese infused rats. Each pixel in the image was fit to extract an R1 map for each rat. The maps were then registered and averaged. Figure 6B displays the difference between the average R1 map for the $MnCl_2$ group and the average R1 map for the saline group, ie, the "Mn" map. Figures 6C and 6D show a representative coronal map and the averaged coronal "Mn" map. The water samples are seen in Figure 6C but have been cropped in Figure 6D as they were not in identical location between different rats and thus could not be registered. All regions of the brain had significantly ($P < .05$) higher values of R1. As was expected, the greatest change in R1, and thus the highest concentration of Mn^{2+}, was found in the pituitary gland. This location is an entry route to the brain

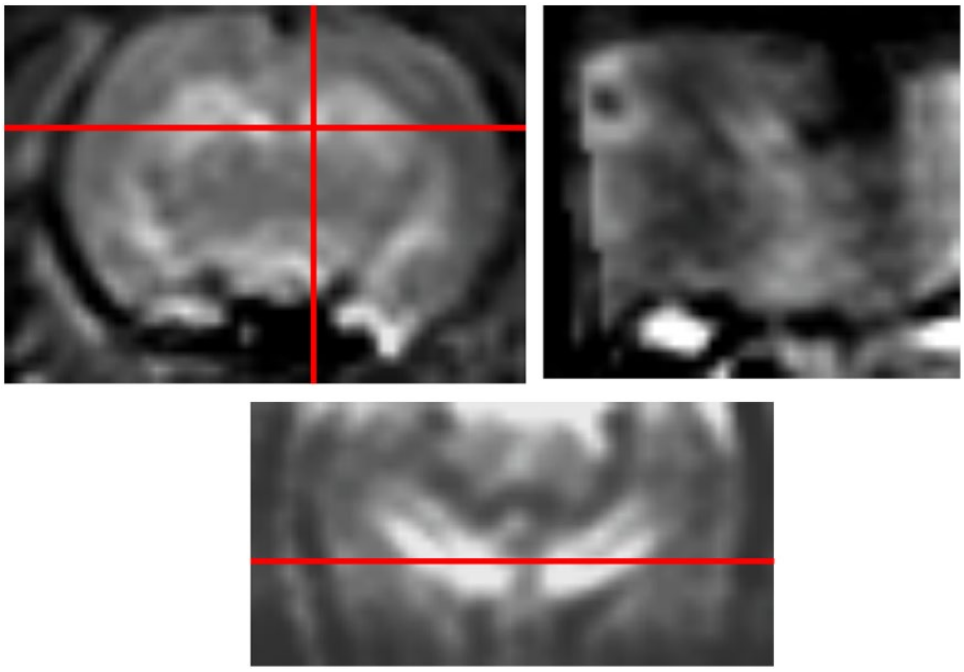

Figure 7. Three orthogonal views from the 3D group-averaged difference. The crosshairs in the coronal (top left) view indicate the locations of the sagittal (right) and horizontal (bottom) slices. The line in the horizontal slice indicates the location of the coronal image. The signal in the water samples (cropped) has been used to normalize the signal of each rat prior to averaging and subtracting (Mn-Sal) the group. Higher signal intensities are proportional to locations of higher Mn concentration or higher relaxivity. Note that only a section of the sagittal direction is excited by the thick slab select pulse, and thus, only part of the brain is visible. The bright region is the pituitary gland.

as the pituitary gland lacks a blood-brain barrier (BBB). Manganese was distributed to the other parts of the brain including the motor system. A more detailed distribution was seen in the 3D MRI images. Figure 7 displays 3 orthogonal slices from the group-averaged difference between the 3D images of the $MnCl_2$ and saline groups. The cerebellum and the olfactory bulbs are not visible as they were not excited by the 12-mm slab excitation. The slab excitation was used to prevent folding in the third dimension while reducing the number of phase-encoding steps and time necessary to achieve isotropic voxels. Each 3D image has been registered. To account for differences in session-to-session amplification and in the slice profile, the intensity was normalized to the intensity of the water sample. The images from each group were then averaged. The selected slices in Figure 7 are from the difference between the average $MnCl_2$ group and the average saline group. Because the signal intensity in the 3D images is weighted by R1 and not a measurement of R1, the images in Figure 7 are proportional to the "Mn" maps shown in Figure 6 but not the same. The pituitary in all the images was the brightest as it has the highest relaxation rate (shortest T_1). The pituitary gland is not directly involved in motor control; however, it is a direct indicator of the total brain dose available to affect the motor system. Thus, in the correlative analysis with respect to behavioral measures, the R1 relaxation rate from the pituitary gland has been used.

Correlative analysis: R1 and behavioral measures. To determine whether $MnCl_2$ affected the behavioral measures, data from either the $MnCl_2$ group or combined saline and $MnCl_2$ groups were subjected to bivariate correlation. The correlation was computed between R1 relaxation rate as an independent measure and the variables assessing skilled and gross motor behavior. The $MnCl_2$ effect on motor behavior was transient. Therefore, the correlative analysis between various behavioral measures and R1 was performed only 24 hours after $MnCl_2$ infusion. To account for individual differences in preinfusion performance, the correlation analysis was also performed on the index for total success ($success_{post}/success_{pre}$). The statistical results for the end-point measures in a single pellet reaching task are summarized in Table 3.

Higher R1 correlated with the reduction in the success level following $MnCl_2$ infusion (Figure 8A). Most importantly, the correlation between R1 and the index for total success was also significant when only $MnCl_2$ group was subjected to bivariate analysis ($r = -0.52$; $P < .05$). That is, the rats after $MnCl_2$ infusion were affected in skilled reaching. Moreover, the reduction in the success level was the result of higher $MnCl_2$ level entering the brain (Table 3).

$MnCl_2$ infusion worsened the reaching movement elements of advance, supination II, and release (Table 4). Figure 8B shows the results between R1 and the index of supination II. More importantly, there was a significant deficit in pronation along increase in R1 ($r = 0.77$; $P < .01$) for the $MnCl_2$ group alone (Table 4), ie, decreasing pronation performance with increasing manganese concentration.

Table 3. Correlation between end-point measures and Mn relaxation rate in a single pellet reaching task.

BEHAVIORAL MEASUREMENT	MN GROUP ONLY	COMBINED GROUPS
Success	ns	$r = -0.56^{***}$
Success index	$r = -0.52^{*}$	$r = -0.51^{**}$
First trial success	ns	$r = -0.44^{*}$
First trial success index	ns	$r = -0.38$; $P = .055$
Total reaching attempts	ns	ns
Total reaching attempts index	ns	$r = -0.45^{*}$

* $P \leq .05$; ** $P \leq .01$; *** $P \leq .001$; ns—$P > .05$.

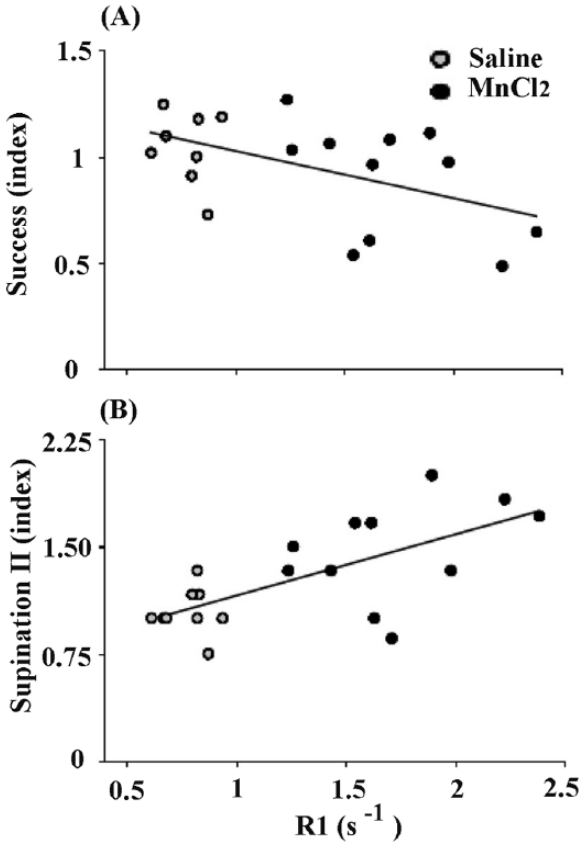

Figure 8. (A) The significant correlation ($P < .05$) between the relaxation rate (R1) in pituitary gland and success index and (B) significant correlation ($P < .05$) between the relaxation rate (R1) in pituitary gland and supination II index 24 hours after infusion. Success and supination II scores were normalized relative to the preinfusion performance (performance index).

Discussion

Magnetic resonance imaging using $MnCl_2$ as a contrast agent has been used as a tool for functional imaging of behavior in healthy rodents and rodents following brain injury. Although manganese is known to produce motor abnormalities at high doses, its use as an image enhancement tool for studying neuronal circuits continues to grow. With lower doses, it has been reported that meaningful image enhancement is achievable free of detectable running wheel[34] and swimming[6] motor abnormalities. This study investigated the effect of a single intravenous infusion of $MnCl_2$ on behavioral tests of fine motor paw function, balancing in a cylinder task, and open field test of general activity. The general expectation from the MEMRI literature is up to 24 hours of lethargy.[29] At 95 mg/kg, this was most certainly the case with the rats not recovering. At the moderate dose of 48 mg/kg, the rats could not be classified as lethargic. Nevertheless, the activity and balance test results showed small but detectable abnormalities that were present more than 24 hours and dissipated more than 3 days. The fact that $MnCl_2$-induced deficits were transient is consistent with previous findings of a transient Mn^{2+}-induced learning deficit in rodents.[23]

The transient nature of Mn^{2+}-induced toxicity is a critical point with respect to longitudinal studies combining MEMRI with investigations on freely behaving animals. Our results demonstrate that careful analysis of behavior is required in assessing impairment. Although end-point measures were spared, more detailed measures on movement elements revealed impairment. Notably, the rats were unable to make rotatory movements at wrist and shoulder when they withdrew the paw with a food pellet to the mouth for eating. They used body movements to compensate for abnormalities, and the compensation allowed them to be as successful as control rats. The rats were also impaired in placing the food item into the mouth and replacing the paw on the substrate after releasing the food. Thus, the results show that after a 48 mg/kg dose of $MnCl_2$, motor skills are detectably altered up the third day after infusion. For most behavioral studies in which the objective is to image brain changes associated with behavior, this is a large time frame. The results are in agreement with the work by Eschenko et al,[4] who detected abnormalities at 80 and 16 mg/kg of $MnCl_2$. Reports of experiments free of detectable abnormalities[34] used slow-release osmotic pumps. Osmotic pumps enable direct brain infusion as an option. This enables a high dose delivery that may reverse the MRI contrast[55]; however, histology follow-up is necessary to distinguish contrast reversal from dead tissue due to the direct infusion.[56] MEMRI dose is a balance between image enhancement and toxicity. Although osmotic pumps may

Table 4. Correlation between behavioral measures and Mn relaxation rate.

BEHAVIORAL TASK	BEHAVIORAL MEASUREMENT	MN GROUP ONLY	COMBINED GROUPS
Single pellet reaching	Advance index	ns	ρ = 0.41*
	Supination II index	ns	ρ = 0.60*
	Release index	ns	ρ = 0.49*
	Pronation	ρ = 0.77**	ρ = 0.40*
	Supination I	ns	ρ = 0.40*
	Supination II	ns	ρ = 0.63*
	Release	ns	ρ = 0.47*
Activity box	Distance covered	NA	ρ = −0.43*
	Number of rears	NA	ρ = −0.48*
Cylinder	Number of rears	NA	ρ = −0.52*
	Rears without support	NA	ρ = −0.46*
	Rears with support	NA	ns

Abbreviation: NA, not applicable.
*$P \leq .05$; **$P \leq .01$; ns—$P > .05$.

have an advantage from a safe delivery point of view, their size puts a limit on the osmolarity-matched dose that can be delivered.[57]

Signal enhancement 24 hours after $MnCl_2$ infusion in brain regions has been suggested to be the result of transport of Mn^{2+} via cerebrospinal fluid (CSF). The choroid plexus[8] has been shown as a predominant route of Mn^{2+} transport at high plasma concentration of Mn^{2+}.[58] The regional distribution of Mn^{2+} in the brain after chronic administration is reported to be quite different with the highest regional concentration observed in the striatum.[29,30] In this study, the midline sagittal slice of Figure 6 shows a crescent-shaped region of brightness curving up from just in front of the pituitary gland. The slice thickness of this image is 1.6 mm. By looking at the rat atlas[53] and the slices that would cover this region around the midline, this intensity follows the shape of the third ventricle. The slices from the 3D MRI images in Figure 7 show that the manganese-enhanced intensity extends into the hippocampal regions but is not as intense in the striatum. The pattern of enhancement in the images suggests that transport is from the blood supply to the pituitary gland, into the CSF, and then to the regions near the ventricles, ie, the hippocampus. Recently, accumulation of Mn^{2+} was reported in other subcortical structures such as hypothalamus and thalamus where the BBB is weak.[59,60]

The high MRI signal in the pituitary gland has been previously reported.[29,46] The imaging data and previous literature support the hypotheses of the pituitary gland being an integral part of the circulation of $Mn^{2+}$to the brain. Although the pituitary gland is not directly involved in motor control, the R1 measurements from the pituitary gland are indicators of the total brain dose available to affect the motor system. In addition, this measure accounts for any differences in blood volume or experimental errors in the infusion procedure and is an easy feature to describe from in a single brain slice. The most interesting findings of this work are the correlations between R1 in the pituitary gland and multiple measures of fine motor skill performance. For some of the performance measures, a higher value is an indicator of better performance, whereas in others lower values are better. In all cases, the sign of the correlation with R1 was such that higher R1 (more Mn) resulted in poorer performance.

The induced abnormalities in skilled and gross motor behavior are likely attributable to Mn^{2+} accumulations in brain regions contributing to motor behavior. The MRI signal was enhanced in all regions including the cortex, subcortical structures, and cerebellum. All of these brain regions are involved in the motor behavior assessed in this study.[61,62] For example, the cerebellum[63] and dopamine-rich brain regions of the striatum[64] are sites of the accumulation of Mn^{2+}, and these structures contribute to skilled reaching, locomotion, and balancing ability. The very specific nature of the motor impairments leads us to believe that they are due to the effects of the Mn^{2+} on the brain.

The 100% mortality rate in the group of rats who received intravenous 95 mg/kg $MnCl_2$ dose is contrary to the literature. One possible reason for the mortality could be the strain of the rats used (Long Evans).[6] The rats used in this study are larger than those generally used in the imaging MEMRI literature and thus requiring longer total infusion times, making the infusion process more challenging. Our observation suggests that tail vein infusion of $MnCL_2$ in adult rats is a complicated procedure and alternative methods should be employed except

in special circumstances. Other complicating factors could be rat gender and route of infusions or the use of Bicine as a buffer. Further investigation is needed to determine factors contributing to mortality.

In conclusion, this study reveals that a single 48 mg/kg $MnCl_2$ dose produces behavioral changes that last up to 3 days. In assessing possible $MnCl_2$ toxicity, it is advisable to use multiple measures of behavior and to use assessments of the way that movements are performed in addition to end-point measures. In combined studies of behavior and MEMRI with acute single doses, deficits are likely to occur, and carefully controlled experiments to avoid behavioral confounds are necessary. Achieving adequately enhanced MEMRI images while having rats free of detectable deficits likely requires single systemic doses lower than 48 mg/kg of $MnCl_2$ or an alternate delivery strategy.

Acknowledgements

The authors would like to acknowledge Jaden Wright, Scott Robson, and James Cardiff for their assistance with the animal training and data collection for this project.

Author Contributions

ARC conceived experiments and designed and tested MRI protocol, coil, and analysis software. ARC and MA designed experiments, wrote the first draft of the manuscript, jointly developed the structure and arguments for the paper, and made revisions to address the reviewers' comments. ARC, MA, and VL analyzed the data. ARC, MA, and IQW contributed to the writing of the manuscript. ARC, MA, VL, and IQW agree with manuscript results and conclusions. ARC, MA, and IQW made critical revisions to the final version. All authors reviewed and approved the final manuscript.

Disclosures and Ethics

The experiments were conducted in compliance with the guidelines and approval of the "University of Lethbridge Animal Care Committee" (Institutional Ethical Committee). The "University of Lethbridge Animal Care Committee" follows the setting and maintaining standards for the ethical use and care of animals in science in Canada by the "Canadian Council for Animal Care" (CCAC) which reflect international guidelines.

REFERENCES

1. Lin YJ, Koretsky AP. Manganese ion enhances T1-weighted MRI during brain activation: an approach to direct imaging of brain function. *Magn Reson Med*. 1997;38:378–388.
2. Bissig D, Berkowitz BA. Manganese-enhanced MRI of layer-specific activity in the visual cortex from awake and free-moving rats. *Neuroimage*. 2009;44:627–635.
3. Boretius S, Frahm J. Manganese-enhanced magnetic resonance imaging. *Methods Mol Biol*. 2011;771:531–568.
4. Eschenko O, Canals S, Simanova I, Beyerlein M, Murayama Y, Logothetis NK. Mapping of functional brain activity in freely behaving rats during voluntary running using manganese-enhanced MRI: implication for longitudinal studies. *Neuroimage*. 2010;49:2544–2555.
5. Inoue T, Majid T, Pautler RG. Manganese enhanced MRI (MEMRI): neurophysiological applications. *Rev Neurosci*. 2011;22:675–694.
6. Jackson SJ, Hussey R, Jansen MA, et al. Manganese-enhanced magnetic resonance imaging (MEMRI) of rat brain after systemic administration of $MnCl_2$: hippocampal signal enhancement without disruption of hippocampus-dependent behavior. *Behav Brain Res*. 2011;216:293–300.
7. Silva AC. Using manganese-enhanced MRI to understand BOLD. *Neuroimage*. 2012;62:1009–1013.
8. Aoki I, Wu YJ, Silva AC, Lynch RM, Koretsky AP. In vivo detection of neuroarchitecture in the rodent brain using manganese-enhanced MRI. *Neuroimage*. 2004;22:1046–1059.
9. Allegrini PR, Wiessner C. Three-dimensional MRI of cerebral projections in rat brain in vivo after intracortical injection of $MnCl_2$. *NMR Biomed*. 2003;16:252–256.
10. Canals S, Beyerlein M, Keller AL, Murayama Y, Logothetis NK. Magnetic resonance imaging of cortical connectivity in vivo. *Neuroimage*. 2008;40:458–472.
11. Pautler RG, Silva AC, Koretsky AP. In vivo neuronal tract tracing using manganese-enhanced magnetic resonance imaging. *Magn Reson Med*. 1998;40:740–748.
12. Pautler RG, Mongeau R, Jacobs RE. In vivo trans-synaptic tract tracing from the murine striatum and amygdala utilizing manganese enhanced MRI (MEMRI). *Magn Reson Med*. 2003;50:33–39.
13. Watanabe T, Frahm J, Michaelis T. Functional mapping of neural pathways in rodent brain in vivo using manganese-enhanced three-dimensional magnetic resonance imaging. *NMR Biomed*. 2004;17:554–568.
14. Van der Linden A, Van Meir V, Tindemans I, Verhoye M, Balthazart J. Applications of manganese-enhanced magnetic resonance imaging (MEMRI) to image brain plasticity in song birds. *NMR Biomed*. 2004;17:602–612.
15. Yu X, Wadghiri YZ, Sanes DH, Turnbull DH. In vivo auditory brain mapping in mice with Mn-enhanced MRI. *Nat Neurosci*. 2005;8:961–968.
16. Drapeau P, Nachshen DA. Manganese fluxes and manganese-dependent neurotransmitter release in presynaptic nerve endings isolated from rat brain. *J Physiol*. 1984;348:493–510.
17. Narita K, Kawasaki F, Kita H. Mn and Mg influxes through Ca channels of motor nerve terminals are prevented by verapamil in frogs. *Brain Res*. 1990;510:289–295.
18. Chuang KH, Koretsky AP, Sotak CH. Temporal changes in the T1 and T2 relaxation rates (DeltaR1 and DeltaR2) in the rat brain are consistent with the tissue-clearance rates of elemental manganese. *Magn Reson Med*. 2009;61:1528–1532.
19. Rovetta F, Catalani S, Steimberg N, et al. Organ-specific manganese toxicity: a comparative in vitro study on five cellular models exposed to $MnCl_2$. *Toxicol Vitro*. 2007;21:284–292.
20. Silva AC, Bock NA. Manganese-enhanced MRI: an exceptional tool in translational neuroimaging. *Schizophr Bull*. 2008;34:595–604.
21. Crossgrove J, Zheng W. Manganese toxicity upon overexposure. *NMR Biomed*. 2004;17:544–553.
22. Gwiazda R, Lucchini R, Smith D. Adequacy and consistency of animal studies to evaluate the neurotoxicity of chronic low-level manganese exposure in humans. *J Toxicol Environ Health A*. 2007;70:594–605.
23. Oner G, Senturk UK. Reversibility of manganese-induced learning defect in rats. *Food Chem Toxicol*. 1995;33:559–563.
24. Ono K, Komai K, Yamada M. Myoclonic involuntary movement associated with chronic manganese poisoning. *J Neurol Sci*. 2002;199:93–96.
25. Vezer T, Papp A, Hoyk Z, Varga C, Naray M, Nagymajtenyi L. Behavioral and neurotoxicological effects of subchronic manganese exposure in rats. *Environ Toxicol Pharmacol*. 2005;19:797–810.
26. Wang JD, Soong WT, Chao KY, Hwang YH, Jang CS. Occupational and environmental lead poisoning: case study of a battery recycling smelter in Taiwan. *J Toxicol Sci*. 1998;23:241–245.
27. Witholt R, Gwiazda RH, Smith DR. The neurobehavioral effects of subchronic manganese exposure in the presence and absence of pre-parkinsonism. *Neurotoxicol Teratol*. 2000;22:851–861.
28. Sepulveda MR, Dresselaers T, Vangheluwe P, et al. Evaluation of manganese uptake and toxicity in mouse brain during continuous $MnCl_2$ administration using osmotic pumps. *Contrast Media Mol Imaging*. 2012;7:426–434.
29. Silva AC, Lee JH, Aoki I, Koretsky AP. Manganese-enhanced magnetic resonance imaging (MEMRI): methodological and practical considerations. *NMR Biomed*. 2004;17:532–543.
30. Gallez B, Baudelet C, Geurts M. Regional distribution of manganese found in the brain after injection of a single dose of manganese-based contrast agents. *Magn Reson Imaging*. 1998;16:1211–1215.
31. Roels H, Meiers G, Delos M, et al. Influence of the route of administration and the chemical form ($MnCl_2$ MnO_2) on the absorption and cerebral distribution of manganese in rats. *Arch Toxicol*. 1997;71:223–230.
32. Barbeau A. Manganese and extrapyramidal disorders (a critical review and tribute to Dr.George C. Cotzias). *Neurotoxicology*. 1984;5:13–35.

33. Calabresi P, Ammassari-Teule M, Gubellini P, et al. A synaptic mechanism underlying the behavioral abnormalities induced by manganese intoxication. *Neurobiol Dis*. 2001;8:419–432.
34. Eschenko O, Canals S, Simanova I, Logothetis NK. Behavioral, electrophysiological and histopathological consequences of systemic manganese administration in MEMRI. *Magn Reson Imaging*. 2010;28:1165–1174.
35. Van der Linden A, Van Camp N, Ramos-Cabrer P, Hoehn M. Current status of functional MRI on small animals: application to physiology, pathophysiology, and cognition. *NMR Biomed*. 2007;20:522–545.
36. Alaverdashvili M, Whishaw IQ. A behavioral method for identifying recovery and compensation: hand use in a preclinical stroke model using the single pellet reaching task. *Neurosci Biobehav Rev*. 2013;37:950–967.
37. Whishaw IQ, Pellis SM. The structure of skilled forelimb reaching in the rat: a proximally driven movement with a single distal rotatory component. *Behav Brain Res*. 1990;41:49–59.
38. Brimblecombe RW. Effects of psychotropic drugs on open-field behavior in rats. *Psychopharmacologia*. 1963;4:139–147.
39. Schallert T, Fleming SM, Leasure JL, Tillerson JL, Bland ST. CNS plasticity and assessment of forelimb sensorimotor outcome in unilateral rat models of stroke cortical ablation Parkinsonism and spinal cord injury. *Neuropharmacology*. 2000;39:777–787.
40. Moon SK, Alaverdashvili M, Cross AR, Whishaw IQ. Both compensation and recovery of skilled reaching following small photothrombotic stroke to motor cortex in the rat. *Exp Neurol*. 2009;218:145–153.
41. Gharbawie OA, Whishaw IQ. Parallel stages of learning and recovery of skilled reaching after motor cortex stroke: "oppositions" organize normal and compensatory movements. *Behav Brain Res*. 2006;175:249–262.
42. Eshkol N, Wachmann A. *Movement Notation*. London, England: Weidenfeld & Nicolson; 1958.
43. Whishaw IQ, Gorny B. Arpeggio and fractionated digit movements used in prehension by rats. *Behav Brain Res*. 1994;60:15–24.
44. Alaverdashvili M, Foroud A, Lim DH, Whishaw IQ. "Learned baduse" limits recovery of skilled reaching for food after forelimb motor cortex stroke in rats: a new analysis of the effect of gestures on success. *Behav Brain Res*. 2008; 188:281–290.
45. Foroud A, Whishaw IQ. Changes in the kinematic structure and non-kinematic features of movements during skilled reaching after stroke: a Laban Movement Analysis in two case studies. *J Neurosci Methods*. 2006;158:137–149.
46. Lee JH, Silva AC, Merkle H, Koretsky AP. Manganese-enhanced magnetic resonance imaging of mouse brain after systemic administration of $MnCl_2$: dose-dependent and temporal evolution of T1 contrast. *Magn Reson Med*. 2005;53:640–648.
47. Koretsky AP. Is there a path beyond BOLD? Molecular imaging of brain function. *Neuroimage*. 2012;62:1208–1215.
48. Ingersoll RT, Montgomery EB Jr, Aposhian HV. Central nervous system toxicity of manganese. I. Inhibition of spontaneous motor activity in rats after intrathecal administration of manganese chloride. *Fundam Appl Toxicol*. 1995;27:106–113.
49. Bradbury M. *The Concept of a Blood-Brain Barrier*. Chichester, UK: John Wiley & Sons; 1979.
50. Kuo YT, Herlihy AH, So PW, Bhakoo KK, Bell JD. In vivo measurements of T1 relaxation times in mouse brain associated with different modes of systemic administration of manganese chloride. *J Magn Reson Imaging*. 2005;21:334–339.
51. Smith QR, Rapoport SI. Cerebrovascular permeability coefficients to sodium, potassium, and chloride. *J Neurochem*. 1986;46:1732–1742.
52. Hoult DI. The NMR Receiver: a description and analysis of design. *Prog NMR Spectrosc*. 1978;12:41–77.
53. Paxinos G, Watson CH. *The Rat Brain in Stereotaxic Coordinates*. Burlington, NJ: Academic Press; 2007.
54. Field AP, Hole GP. *How to Design and Report Experiments*. London, England: SAGE; 2003.
55. Seo Y, Takamata A, Ogino T, Morita H, Murakami M. Lateral diffusion of manganese in the rat brain determined by T(1) relaxation time measured by (1)H MRI. *J Physiol Sci*. 2011;61:259–266.
56. McCreary JK. *Applications of Manganese-Enhanced Magnetic Resonance Imaging in Neuroscience* [MSc thesis]. Lethbridge, AB: University of Lethbridge; 2012.
57. McCreary JK, Truica LS, Friesen B, et al. Altered brain morphology and functional connectivity reflect a vulnerable affective state after cumulative multigenerational stress in rats. *Neuroscience*. 2016;330:79–89.
58. Aschner M, Dorman DC. Manganese: pharmacokinetics and molecular mechanisms of brain uptake. *Toxicol Rev*. 2006;25:147–154.
59. Huber JD, VanGilder RL, Houser KA. Streptozotocin-induced diabetes progressively increases blood-brain barrier permeability in specific brain regions in rats. *Am J Physiol Heart Circ Physiol*. 2006;291:H2660–H2668.
60. Kuo Y-T, Herlihy AH, So P-W, Bell JD. Manganese-enhanced magnetic resonance imaging (MEMRI) without compromise of the blood-brain barrier detects hypothalamic neuronal activity in vivo. *NMR Biomed*. 2006;19: 1028–1034.
61. Tennant KA, Adkins DL, Scalco MD, et al. Skill learning induced plasticity of motor cortical representations is time and age-dependent. *Neurobiol Learn Mem*. 2012;98:291–302.
62. Young NA, Vuong J, Teskey GC. Development of motor maps in rats and their modulation by experience. *J Neurophysiol*. 2012;108:1309–1317.
63. Chen MT, Cheng GW, Lin CC, Chen BH, Huang YL. Effects of acute manganese chloride exposure on lipid peroxidation and alteration of trace metals in rat brain. *Biol Trace Elem Res*. 2006;110:163–178.
64. Newland MC. Animal models of manganese's neurotoxicity. *Neurotoxicology*. 1999;20:415–432.